Chemical and Process Engineering Research
ISSN 2224-7467 (Paper) ISSN 2225-0913 (Online)
Vol.19, 2014

Analytical Profile of 4 - (4-Nitro Benzene Azo) - 3 - Amino Benzoic Acid on a Surface of Natural Granulated Calcined Iraqi Montmorillonite Clay Mineral, via Columnar Method.

Mohammed H. Abdul Latif [a *], Mohammed A.K. Alsouz [b], Ibtisam J. Dawood [c], Amer J. Jarad [d].
[a, c, d.] Department of Chemistry, Ibn Al Haitham College of Education, University of Baghdad , Adhamiya, Al-Dilal Square, Baghdad, Iraq.
[b.] Chemistry department, College of science, Al- Mustansiriya University, Al- Mustansiriya, Baghdad, Iraq
Email: mohammed21latif@yahoo.com
Mobil: +9647901198288

Abstract
The adsorption ability of Iraqi initiated calcined granulated montmorillonite to adsorb of 4-(4-Nitrobenzeneazo) 3-Aminobenzoic Acid from aqueous solutions has been investigated through columnar method. The azo dye adsorption found to be dependent on adsorbent dosage, initial concentration and contact time. All columnar experiments were carried out at three different pH values (5.5, 7and 8) using buffer solutions at flow rate of (3 drops/ min.), at room temperature (25±2) °C. The experimental isotherm data were analyzed using Langmuir, Freundlich and Temkin equations. The monolayer adsorption capacity is 6.4066 mg Azo ligand per 1g calcined Montmorillonite. The experiments showed that highest removal rate 90.5 % for azo dye at pH 5.5.The kinetic data for the adsorption process obeyed pseudo-first -order rate equations.
Keywords: Analytical profile, Azo Ligand, Iraqi Montmorillonite, Columnar Method., Calcined.

1. Introduction

Azo compounds are known for their medicinal importance and are well recognized for their use as antineoplastic [1], antidiabetics [2], antiseptics [3], antibacterial [4, 5], antitumor [6]. They are known to be involved in a number of biological reactions such as inhibition of DNA, RNA and protein synthesis, carcinogenesis and nitrogen fixation [7-8]. Furthermore, azo dye compounds also have a lot of applications in industry and photodynamic therapy as well as photosensitive species in photographic or electro photographic systems and are dominant organic photoconductive materials [6, 9]. Azo compounds are important structures in the medicinal and pharmaceutical fields 10] and it has been suggested that the azoimine linkage might be responsible for the biological activities displayed by some reported Schiff bases [11, 12]. In addition, Evans blue and Congo red are azo dyes being studied as HIV inhibitors of viral replications. This effect is believed to be caused by binding of azo dyes to both protease and reverse transcriptase of this virus [13]. The existence of an azo moiety in different types of compounds has caused them to show antibacterial and pesticidal activities. In the recent times, exploration of azo dye as antimicrobial agents has received considerable attention [9, 11, 14, and 15]. In the light of variety of diverse applications of azo dyes analytical behavior of 4-(4-Nitrobenzeneazo) - 3-Aminobenzoic Acid has been investigated on the Iraqi mineral clay in the target to be applied as desalinated water disinfectant.
Clay minerals are the most important inorganic components in soil due to their excellent adsorption properties [16]. Natural mineral clays possess specific surface chemical properties, e.g., cation exchange capacity, and adsorptive affinity for some organic and inorganic compounds. Bentonite is an absorbent aluminum phyllosilicate, essentially impure clay consist in mostly of montmorillonite. There are different types of Montmorillonite, each named after the respective dominant element, such as potassium (K), sodium (Na), calcium (Ca), and aluminum (Al) [17]. Montmorillonite clay deposits are mostly composed of clay minerals, a subtype of phyllosilicate minerals, which imparts plasticity and harden when fired or dried [18]. Montmorillonite possess adsorption properties mainly because of their colloidal nature which stems from their very small particle size. The structure of montmorillonite is an octahedral alumina sandwiched between two tetrahedral silica sheets to form the structural unit. Variations in interstitial water and exchangeable cations in the interlayer space affect the properties of Montmorillonite [19]. Vermiculite and Montmorillonite are clay minerals with high CEC. The surface area for west Iraqi bentonite was estimated using methylene blue (MB) adsorption method and it was (123 m^2 /g) [20]. West Iraqi bentonite consists mostly of calcium – montmorillonite. The percent of montmorillonite is between (60 – 65 %) of crude bentonite, (Table 1) show the chemical analysis of west Iraqi Montmorillonite. Therefore it is necessary to remove the impurities before the bentonite is ready to use [21].

Table 1. Chemical analysis of West Iraqi Bentonite.

Compound	SiO_2	Al_2O_3	Fe_2O_3	CaO	MgO	Na_2O	K_2O	LiO_2	SO_3	L.I.O.	Total
Weight %	55.81	14.91	5.78	5.72	3.5	1.29	0.41	0.67	----	10.86	99.67

In this study we investigate the adsorption, of 4-(4-Nitrobenzeneazo) 3-Aminobenzoic Acid prepared by Coupling reaction of 4-nitroaniline with 3-aminobenzoic acid [22], on the surface of calcined initiated Iraqi Montmorillonite clay packed in glass columns, and calculate the effect of factors like pH, ionic strength, contact time, and weight of clay on percentage of removal of the azo ligand, also calculate the isothermic factors of adsorption process.

2. Materials and methods

2.1. Materials

All the chemicals and solvents were of analytical grade (supplied by either Merck or Fluka) received. Distilled and deionized water with conductivity value of 1.5×10^{-5} S cm^{-1} was used in all experiments. Montmorillonite clay mineral obtained from the General Company for Geological Survey and Mining in Baghdad, Iraq. The samples were sieved to produce the desired particle size fractions. The samples with a particle size 45µm was then dried for 24 h at 110 ºC in an electric oven and stored in a desiccator until use.

2.2. *General procedure for the Preparation of 4 - (4-Nitrobenzeneazo) - 3 - Amino benzoic Acid ligand.*

According to a known general method [23], 4-nitroaniline (0.342 g, 1 m mole) was dissolved in a mixture of sulphuric acid (2 ml), ethanol (10 ml) and distilled water (10 ml), and diazotized at 5 ºC with sodium nitrite solution. The diazo solution was added drop wise with stirring to a cooled ethanolic solution of 3-amino-benzoic acid (0.345 g, 1 m mole). 25 ml of 1 M sodium hydroxide solution was then added to the dark colored mixture. The precipitate was filtered off and washed several times with 1:1 ethanol: water mixture, then left to dry. The reaction is shown in Scheme 1, while Table 2 describes the physical properties and elemental analysis [22].

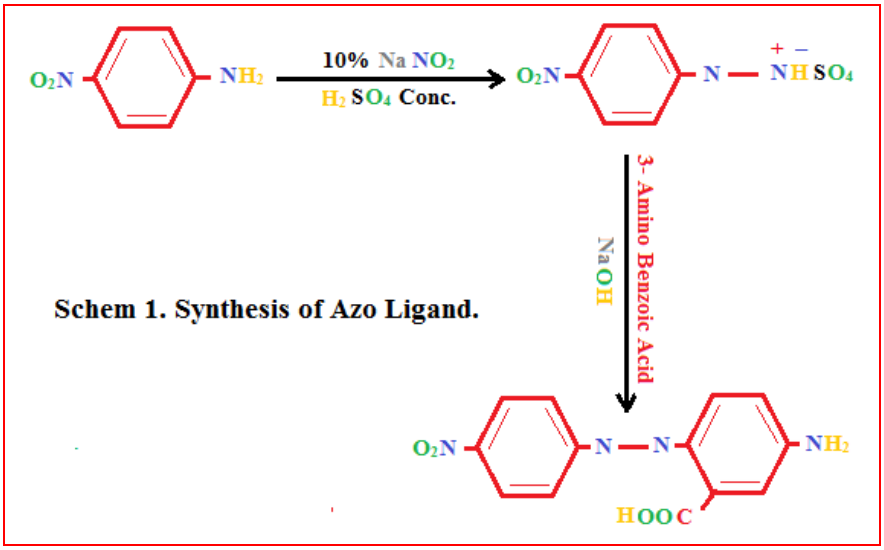

Scheme (1): Schematic representation of synthesis of azo ligand.

Table 2. Physical Properties and Elemental Analysis of Azo Ligand.

Compounds	Color	M.P. ºC	Yield %	Analysis Calculated (Found)			
				M	C %	H %	N %
Ligand (L)	Orange	224	77	-	54.54	3.49	19.58
					(53.65)	(3.21)	(18.53)

2.3. Preparation of buffer and stock solutions.

Three phthalate and phosphate buffer solutions of pH values (5.5, 7, and 8) were prepared respectively [24], also a three stock solutions of the prepared azo ligand of 2000 mg /L concentration were prepared in 100 ml volumetric flask using the above buffer solutions.

2.5. Procedure for synthesis of granulated Iraqi calcined Initiated Na – montmorillonite clay.

In this study the bentonite was beneficiated to improve its Smectite (Montmorillonite) content by attrition – scrubbing at high solid concentration (50%) and at high impeller speed (2500 r.p.m.) for 1 h, using flotation cell. In order to convert calcium - montmorillonite to sodium - montmorillonite the process performed by mixing the bentonite preconcentrate with Na – form activated amberlight orange ion exchanger followed by agitation for 1

h, at 150 r.p.m. The clay was separated from the mixture by filtration, washed five times with distilled water. Each washing step involved stirring the slurry in distilled water, followed by centrifugation and removal of the supernant, the obtained Na – montmorillonite finally treated with 0.5 M NaCl to ensure complete transformation to the Na – form, then the treated clay was washed with distilled water to remove excess NaCl, turned to a granules of (2mm) diameter using granulating machine (GK Dry Granulating Machine) and dried at 110 ^{o}C for 3h, until constant mass, and then burned at 650^{o}C to make an ion – exchange column ready to use

2.6. Columnar adsorption procedure.

Three standard solutions of azo ligand 30 mg /L concentration were prepared from stock solutions of the ligand in different pH values (5.5, 7and 8) using buffer solutions. UV-Visible scanning spectrum has been recorded using (UV-Vis – 1800 Shimadzu Spectrophotometer) and wavelength values corresponding to the maximum absorption found to be at (399 nm for pH = 5.5), (400 nm for pH = 7), and (401 nm for pH = 8), as shown in (Figure 1), (Figure 2), and (Figure 3) respectively, these values choosed for measurements of estimation throughout this research.

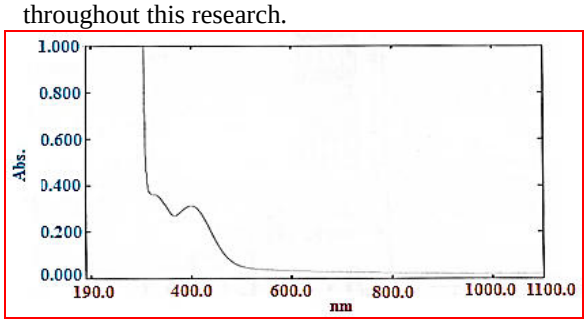

Figure 1. Scanning graph of Azo Ligand, Buffer soln. pH = 5.5, Conc. = 30 ppm. At λ max. = 399 nm.

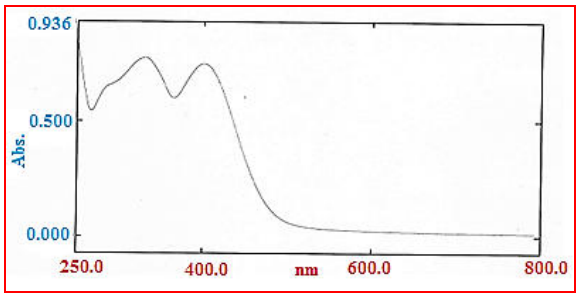

Figure 2. Scanning graph of Azo Ligand, Buffer soln. pH =7, Conc.= 30 ppm., at λ max. = 400 nm.

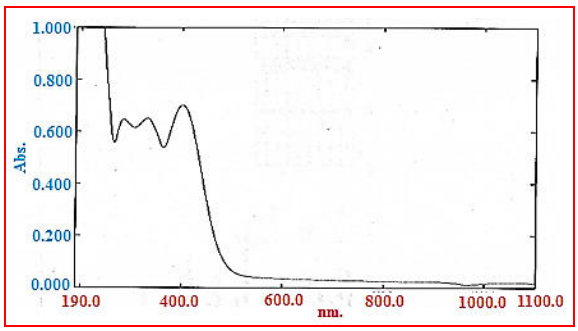

Figure 3. Scanning graph of Azo Ligand, Buffer soln. pH = 8, Conc. = 30 ppm. at λ max. = 401 nm.

Seven standard solutions of azo ligand in the range of (5 - 35 mg /L) concentrations were prepared from stock solutions of azo ligand at different pH values (5.5, 7and 8) using buffer solutions. The absorbance of each solution was measured at λ max. (399 nm for pH = 5.5), (400 nm for pH = 7), and (401 nm for pH = 8) respectively against blank (buffer solution corresponding to pH value). A calibration curves were drown between absorbance and concentration of azo ligand standard solutions, as shown in (Figure 4), (Figure 5), and (Figure 6) respectively.

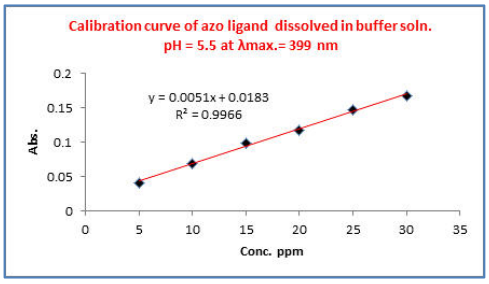

Figure 4. Calibration curve of Azo Ligand dissolved in buffer soln. pH = 5.5

at λ max. = 399 nm.

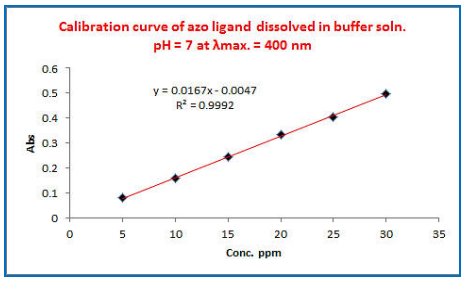

Figure 5. Calibration curve of Azo Ligand dissolved in buffer soln. pH = 7

at λ max. = 400nm.

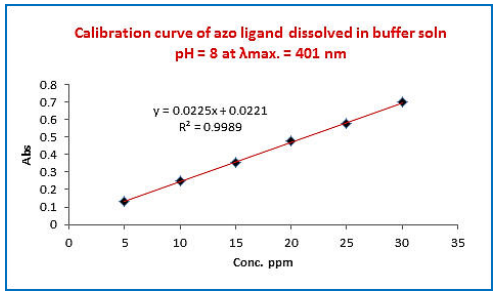

Figure 6. Calibration curve of Azo Ligand dissolved in buffer soln. pH = 8 at λ max. = 401 nm

A six glass columns (50 cm x 10 mm i.d.) filled with known mass (1gm) of natural mineral clay adsorption bed (Initiated Burned Na - montmorillonite) corresponding to bed height of (17 mm) (the surface area of 1 gm. mass of natural clay adsorption bed was calculated physically and its found to be 23.904 c m^2) have been prepared to run (10 ml) of each of (20 – 70 mg/L) azo ligand solutions adjusted to different pH values (5.5, 7and 8) using buffer solutions at flow rate of (3 drops/ min.), at room temperature (25±2) °C. Then we examined the percolated solutions by measuring the absorbance of each solution at fixed λ max., that have been identified for each pH value, using (UV-Vis – 1800 Shimadzu Spectrophotometer).The equilibrium adsorption uptake q_e (mg/g) and percent removal of azo ligand from the aqueous solution was calculated using the relationship noted at the bottom of the (Table 3).

Table 3. Adsorption parameters of adsorption of azo ligand on initiated burned Iraqi bentonite clay mineral.

Adsorbate Azo ligand concentration C◦	pH 5.5			pH 7			pH 8		
	C_e	% removal	q_e	C_e	Removal %	q_e	C_e	Removal %	q_e
20	1.90	90.5	0.1810	12.49	37.5	0.0751	11.77	41.5	0.0823
30	5.19	82.5	0.2481	18.72	37.6	0.2128	16.79	44.0	0.1321
40	7.78	80.5	0.3222	20.16	49.7	0.1984	23.81	40.5	0.1619
50	9.35	81.3	0.4065	33.57	33.0	0.1643	36.04	27.9	0.1396
60	21.31	64.5	0.3869	39.08	34.8	0.2092	41.72	30.5	0.1828
70	29.15	58.3	0.4085	41.65	40.5	0.2835	46.88	33.1	0.2312

Amount adsorbed q_e= (C_0-C_e)V/W (mg of adsorbate / g of adsorbent), removal %= 100(C_0-C_e)/ C_e, Where C_0 is the initial sorbate concentration (mg/L), C_e the equilibrium adsorbate concentration (mg/L), V is the volume of solution in L and w is the mass of the adsorbent in (g) [25].

3. Results and discussion

3.1. Characterization of bentonite clay mineral.

Natural Iraqi bentonite was characterized by FT –IR spectroscopic analysis (Shimadzu FTIR Spectrometer – 30 000:1/ IRAff). FT-IR spectrum (Figure 7. A) illustrate absorption band at 3628.10 cm^{-1} (Al-Al-OH) (Mg-OH-Al) corresponding to vibration of structural OH stretching groups coordinating to Al-Al pair or Mg-OH-Al. Adsorbed water gives a broad bands from 4306.29 cm^{-1} to 3533.59 cm^{-1} corresponding to H_2O- stretching vibration . Al, Mg bound water molecules gives H-O-H stretching vibration bond at 1643 cm^{-1}.Also three bands at 1546.91, 1427.32

And 1384.89 cm^{-1} corresponding to H…O...H weak .The complex broad band around 1033 cm^{-1} belongs to Si-O stretching vibration. Two bands at 914.26 cm^{-1} and 837.11 cm^{-1} are most characteristic for quartz. Finally the bands from 420.00 $cm^{-1}$to 516.93 cm^{-1} are related to Al-O-Si, Si-O-Si deformations. Initiated bentonite FT- IR spectrum (Figure 7. B) illustrate the same bands of (Figure 7. A) but with higher transmittance percent and sharper than bands of FT- IR spectrum of natural bentonite. Nevertheless H…O...H weak disappear in this

spectrum. Adsorbed water band appear at 4321.72 cm^{-1}, two bands belong to Al, and Mg bound water molecules observed at 1654.92 cm^{-1} and 1641.42 cm^{-1}. The broad complex band becomes single band at 1039 cm^{-1} belongs to Si-O stretching vibration. Also we observe two bands belongs to Al…OH stretching vibration at 937.04 cm^{-1} and 916.19 cm^{-1} with higher transmittance percent .The quartz characteristics band from 694.37 cm^{-1} to 839.03 cm^{-1} become broader. Finally Al-O-Si, Si-O-Si and Si-O stretching vibration bands from 426.27 cm^{-1} to 522.71 cm^{-1} become sharper and triplet bond [26]. Calcined initiated Iraqi Montmorillonite FT- IR spectrum (Figure 7. C) illustrate the same bands of that in (Figure 7. B) but sharper and with higher transmittance percent , also the band of adsorbed water become a single band at 3421.7 cm^{-1} mostly due to burning process and the same thing happen with band Al, Mg around water molecule stretching vibration also H…O...H weak bands disappear in this spectrum.

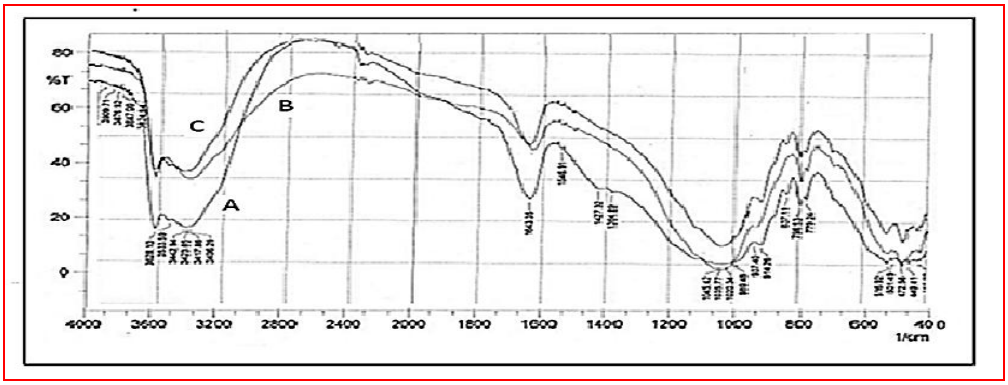

Figure 7. A- FT-IR spectrum for crude west Iraqi bentonite B - FT- IR spectrum for initiated bentonite, C- FT-IR spectrum for burned initiated bentonite

3.2. Calibration graphs.

Three linear calibration curves for azo ligand were obtained at different pH values (5.5, 7and 8) (Figures 4, 5, and 6). Beer's law was obeyed in the concentration range of (5 – 35) mg L^{-1}. Coefficient of determination R^2, Limit of detection (sensitivity) LOD, in addition to other parameters is given in (Table 4).

Table 4.Spectral Characterization and statistical data of the regression equation for Azo Ligand adsorption on calcined Iraqi Montmorillonite.

Parameter	Azo Ligand		
	pH 5.5	pH 7	pH 8
Linearity range (ppm)	5 -35	5 -35	5 -35
Regression equation			
Intercept	0.018267	-0.00473	0.022067
Standard deviation of intercept	0.002857	0.004505	0.007296
slope	0.005051	0.016651	0.022491
Standard deviation of slope	0.000147	0.000231	0.000375
Coefficient of determination R^2	0.996636	0.999228	0.998891
Standard error of Y & X axis STEYX	0.003069	0.004839	0.007837
Limit of detection (sensitivity) LOD	2.004948	0.959063	1.149869
Limit of quantitation LOQ	6.075601	2.906251	3.484452

LOD = 3.3 (STEYX / Slope), LOQ = 10 (STEYX / Slope).

Effect of Adsorbate initial concentration (C◦) of Azo Ligand.

Azo ligand concentrations (20-70 ppm) at different pH values (5.5, 7 and 8) using buffer solutions have been studied on 1g clay bed at room temperature (25±2) °C. Plotting of C_o (initial concentration) values from (Table 3) against Removal % of azo ligand (Figure 8).

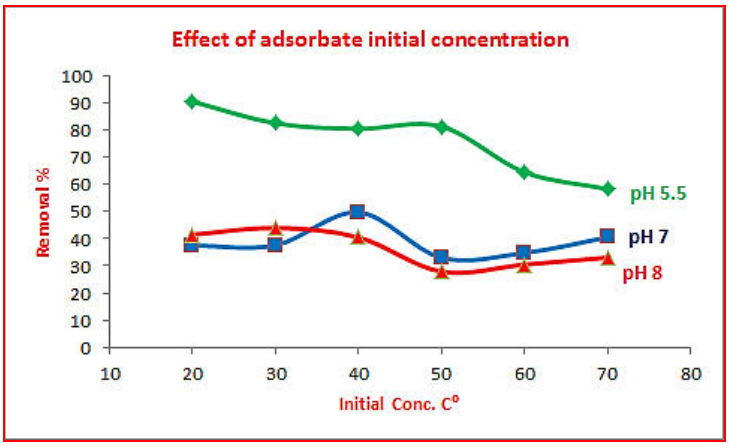

Figure 8. Effect of adsorbate initial concentration of Azo Ligand.

Indicate that the highest adsorption of ligand occurs at PH = 5.5 and the increase in the initial concentration of ligand decreases the removed amount of ligand to the extent that the maximum adsorption capacity of the clay surface attended.

3.3. Effect of pH.

The pH impact on the adsorption of Azo Ligand on the surface of Calcined Initiated Montmorillonite clay examined by preparing three Azo Ligand solutions of constant concentration (20 ppm) adjusted to different pH values (5.5, 7and 8) using buffer solutions. 10 ml of each solution eluted on three columns of 1g clay bed at constant flow rate (3 drops min^{-1}) at room temperature (25±2) °C. The absorbance of these elutes measured and the removal % of Azo Ligand by the clay bed has been calculated. Plotting removal % against the pH values (Figure 9).It's found that the best pH value of adsorption of Azo Ligand on clay bed was (pH = 5.5).

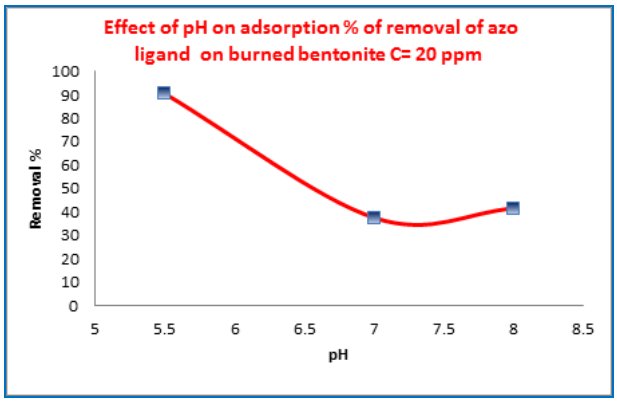

Figure 9. Effect of pH on % of removal of Azo Ligand on Calcined Montmorillonite, C = 20 ppm.

3.4. Effect of clay weight.

Seven different clay weight columns ranged from (1 – 2 g) clay bed were prepared for the elution of (10 ml of 20 ppm concentration) of Azo Ligand solution (pH = 5.5) at constant flow rate of (3 drops/ min.) at room temperature (25±2) °C, then the absorbance of the outlet solutions has been measured, and the removal % of Azo Ligand by the clay bed, calculated and plotted versus the clay weight (Figure 10). It's found that the highest adsorption of Azo Ligand occurs on clay bed of 1.8 g weight. This means adsorption increases with increasing weight of clay to the upper limit of clay capacity, and adsorption surface area.

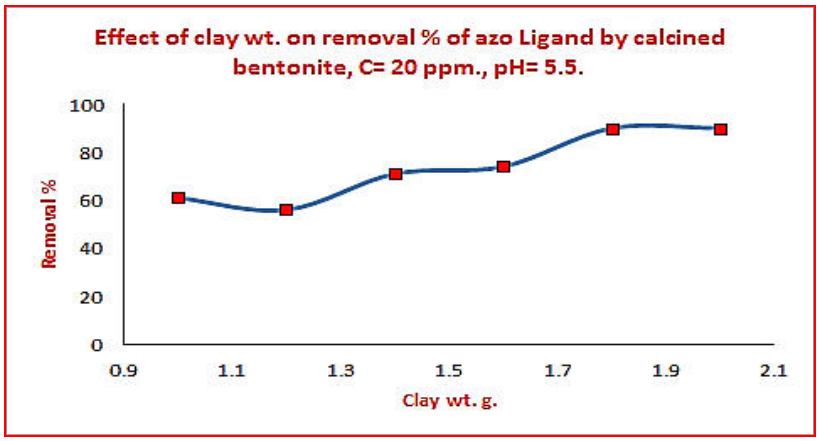

Figure 10. Effect of clay weight on adsorption removal % of Azo Ligand on Calcined Montmorillonite, C = 20 ppm.

3.5. *Effect of ionic strength.*

Ionic strength factor was studied by adding different concentrations (0.1, 0.3, and 0.5M) of sodium chloride solution to three (10 ml of 20 ppm concentration) Azo Ligand solutions. The absorbance's of these solutions run through four adsorption columns of clay bed weight of 2.0 g have been measured. The amounts of ligand adsorbed per unit mass of adsorbent (q_e) (mg/g) has been calculated, and plotted against the molar concentration of NaCl as shown in (Figure 11).It has been noticed that the adsorption increases with the increasing of Na^+ and Cl^- ions concentration on the clay bed surface, which is due to high electrostatic interaction of these ions with the Azo Ligand and that increases Azo Ligand adsorption on the clay surface.

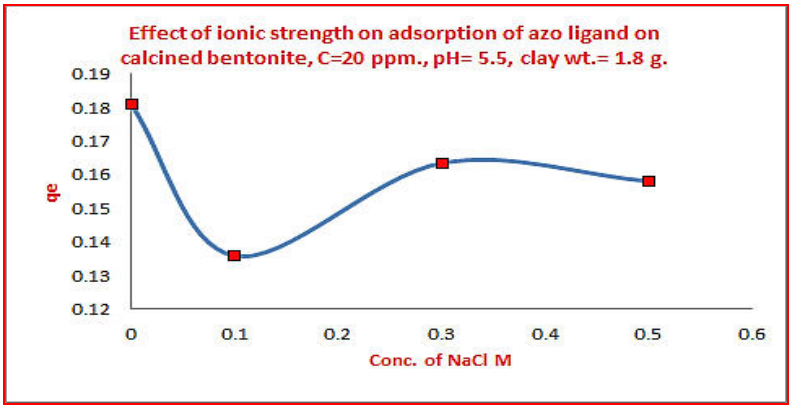

Figure 11. Effect of ionic strength on adsorption of Azo Ligand on Calcined Montmorillonite, C = 20 ppm.

3.8. *Adsorption Isotherms.*

Adsorption isotherms are mathematical models that describe the distribution of the adsorbate species among liquid and adsorbent, based on a set of assumptions that are mainly related to the heterogeneity/homogeneity of adsorbents, the type of coverage and possibility of interaction between the adsorbate species. Adsorption data are usually described by adsorption isotherms, such as Langmuir, Freundlich, and Temkin isotherms [25].The set of experimental results as presented in (Figure 12) at room temperature (25±2) were fitted with the Langmuir, Freundlich, and Temkin models. Adsorption isotherms were obtained and the adsorptive capacity interpreted using both models.

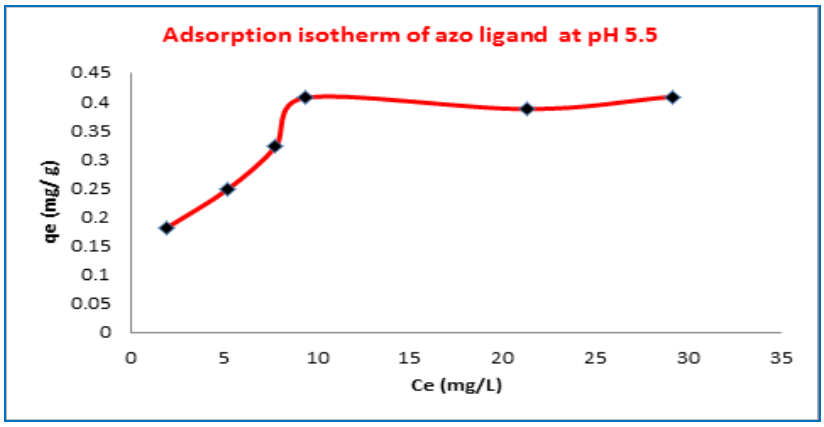

Figure 12. Adsorption isotherm of Azo Ligand at pH = 5.5.

3.8.1. The Langmuir isotherm.

The Langmuir model [27, 28] is based on the assumption that the maximum adsorption occurs when a saturated monolayer of solute molecules is present on the adsorbent surface, the energy of adsorption is constant and there is no migration of adsorbate molecules in the surface plane. The Langmuir isotherm is given by:

$$q_e = \frac{q_m K_L C_e}{1 + K_L C_e} \qquad \text{——— (1)}$$

The constants in the Langmuir isotherm can be determined by plotting (1/*qe*) versus (1/ *Ce*) and making use of above equation rewritten as:

$$\frac{1}{q_e} = \frac{1}{q_m} + \frac{1}{q_m K_L}\frac{1}{C_e} \qquad \text{——— (2)}$$

Where q_m (mg/g) and K_L (L/mg) are the Langmuir constants, representing the maximum adsorption capacity for the solid phase loading and the energy constant related to the heat of adsorption respectively. The values of q_m and K_L can be evaluated from the intercept and the slope of the linear plot of experimental data (Table 5) of ($1/q_e$) versus ($1/C_e$) (Figure 13), and were found to be 6.4066 mg / g and 26.0420 L / mg, respectively. Also the isotherm data fits the Langmuir equation well where the coefficient of determination (R^2 = 0.9275).

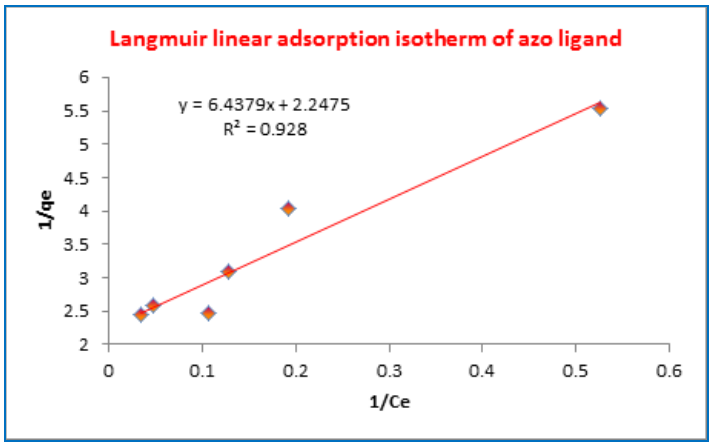

Figure 13. Langmuir linear adsorption isotherm of Azo Ligand.

Table 5.Experimental data of the Adsorption Isotherms.

Adsorbate Azo Ligand concentration C◦	C_e	% removal	Langmuir		Freundlich		Temkin	
			1/Ce	1/ qe	Log q_e	Log C_e	q_e	Ln C_e
20	1.90	90.5	0.5263	5.5248	- 0.7423	0.2787	0.1810	0.6418
30	5.19	82.5	0.1926	4.0306	- 0.6053	0.7151	0.2481	1.6467
40	7.78	80.5	0.1285	3.1036	- 0.4918	0.8909	0.3222	2.0515
50	9.35	81.3	0.1069	2.4600	- 0.3909	0.9708	0.4065	2.2353
60	21.31	64.5	0.0469	2.5846	- 0.4124	1.3285	0.3869	3.0591
70	29.15	58.3	0.0343	2.4479	- 0.3888	1.4646	0.4085	3.3724

3.8.2. The Freundlich isotherm.

The Freundlich isotherm model [29, 30] is an empirical relationship describing the adsorption of solutes from a liquid to a solid surface and assumes that different sites with several adsorption energies are involved. Freundlich adsorption isotherm is the relationship between the amounts of ligand adsorbed per unit mass of adsorbent, q_e, and the equilibrium concentration of ligand C_e.

$$q_e = K_f C_e^{1/n} \qquad \text{——————} (3)$$

The logarithmic form of the equation becomes,

$$\log q_e = \log K_f + \frac{1}{n} \log C_e \qquad \text{——————} (4)$$

Where K_f & n are the Freundlich constants, the characteristics of the system. K_f and n are the indicators of the adsorption capacity and adsorption intensity, respectively. The ability of Freundlich model to fit the experimental data was examined. For this case, the plot of log C_e vs. log q_e was employed to generate the intercept value of K_f and the slope of n. from (Figure 14) .The Freundlich constants K_f and n were found to be 0.1508 and 2.8564 respectively. The Freundlich isotherm is more widely used but provides no information on the monolayer adsorption capacity in contrast to the Langmuir model. Freundlich isotherm fitted well with the coefficient of determination (R^2 = 0.8365).

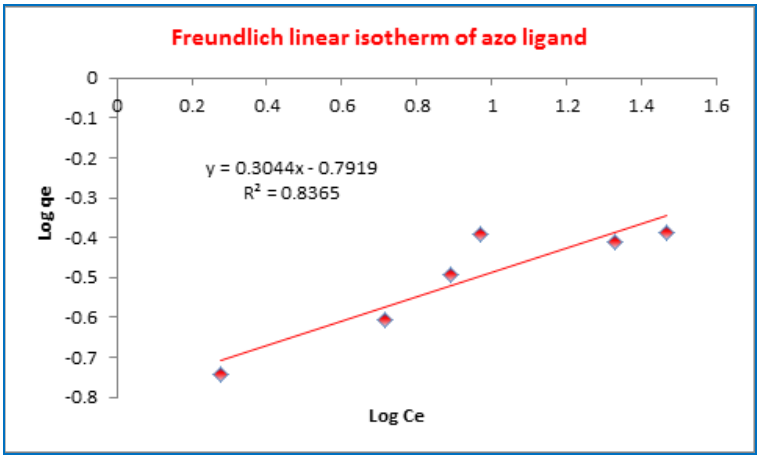

Figure 14. Freundlich linear adsorption isotherm of Azo Ligand.

3.8.3. The Temkin isotherm.

The Temkin isotherm [31] has been used in the following form:

$$q_e = \frac{RT}{b} \ln(AC_e) \qquad \text{——————} \quad (5)$$

A linear form of the Temkin isotherm can be expressed as:

$$q_e = \frac{RT}{b} \ln A + \frac{RT}{b} \ln C_e \qquad \text{——————} \quad (6)$$

$$q_e = B \ln A + B \ln C_e \qquad \text{——————} \quad (7)$$

Where $B = \frac{RT}{b}$, R is gas constant (8.314 J/mol/K), T is Temperature (K)

The sorption data can be analyzed according to Eq. (7). Therefore a plot of q_e versus ln Ce enables one to determine the constants *A* and *B*. The values of the Temkin constants *A* and *B* are listed in Table 1 and the plot of this isotherm is shown in (Figure 15). The coefficient of determination
(R^2 = 0.8279) obtained illustrate that adsorption of Azo ligand also obey Temkin model.

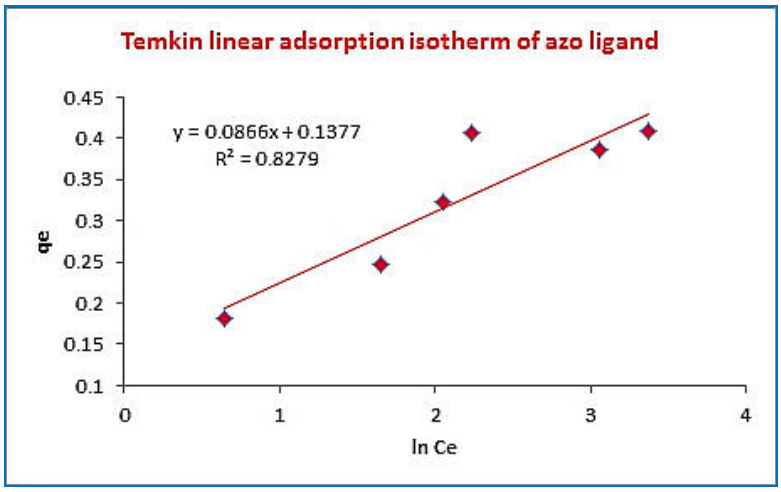

Figure 15.Temkin adsorption isotherm of Ligand (H_2L).

The Langmuir, Freundlich, and Temkin adsorption constants calculated from the corresponding isotherms with the coefficient of determination (R^2) are presented in (Table 6).

Table 6. Isotherm Models Constants and the coefficient of determination (R^2) of Azo Ligand from Aqueous Solution.

Adsorbent	Langmuir isotherm			Freundlich isotherm			Temkin		
Initiated burned Iraqi bentonite clay	q_m (mg/g)	K_L (L/mg)	R^2	K_f	*n*	R^2	*A* (L/g)	*B*	R^2
	6.4066	2.2593	0.9275	0.1508	2.8564	0.8365	4.9041	0.0866	0.8279

3.9. Effect of flow rate (contact time).

Adsorption of Azo ligand was measured at five different flow rates for a (20) ppm concentration of Azo ligand solution. From (Figure 16), the plot reveals that removal percent of Azo ligand is higher at low flow rates. This is probably due to higher contact time at these low flow rates. (Table 7) shows the calculated parameters that illustrate the importance of flow rate and contact time.

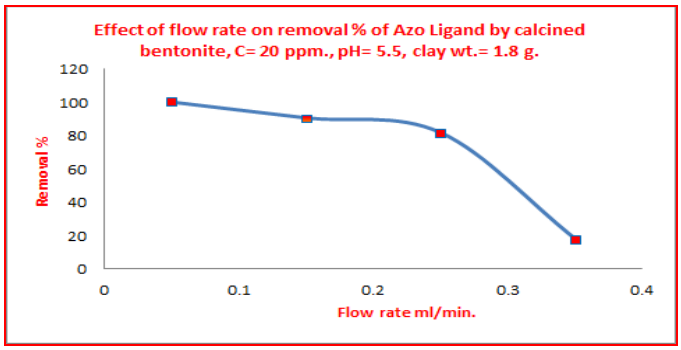

Figure16. Effect of flow rate on adsorption removal % of Azo Ligand on calcined bentonite, C = 20 ppm.

Table 7.Effect of contact time on the adsorption of (20 mg/L) Azo ligand from aqueous solution.

Initial Conc. (mg/L)	Flow rate drop / min	Flow rate ml / min.	*Time(minute)*	Equilibrium Conc. (C_t) (mg/L)	Removal %	q_t (mg/g)	Ln ($q_e - q_t$)	t/q_t	Equilibrium Time(minute)
20	2	0.10	100.00	1.900	90.05	0.1810			66.666
	3	0.15	66.666	1.900	90.50	0.1810		368.3204	
	5	0.25	40.000	3.666	81.66	0.1633	- 4.03419	244.9479	
	7	0.35	28.571	16.411	17.94	0.0358	- 1.92964	798.0726	
	9	0.45	22.222	17.098	14.51	0.0290	-1.88387	985.2068	

3.10. Adsorption kinetics.

Kinetic models are used to examine the rate of the adsorption process in the present work; the kinetic data obtained from the studies have been analyzed by using pseudo-first-order and pseudo-second-order models.
The first order equation of Lagergren is generally expressed as follows.

$dq/dt = k_1 (q_e - q_t)$

Where q_e is the amount of Azo Ligand adsorbed at equilibrium (mg/g), qt is the amount of Azo Ligand adsorbed at time t (min.), and k_1 is the rate constant of pseudo – first - order adsorption. If it supposed that q = 0 at t = 0, then:

$\ln (q_e - q_t) = \ln q_e - k_1 t$
The pseudo-second-order kinetic rate equation is expressed as follows.

$dqt/dt = k_2 (q_e - q_t)^2$

Where k_2 is the rate constant of pseudo-second-order sorption (g/mg/min). The integrated form of Equation when ($t = 0 \rightarrow t$ and $q_t = 0 \rightarrow 0 q_e$) the following expression is obtained:

$t/q_t = 1/k_2 q_e^2 + t/q_e$
The rate constant k_1, k_2 and qe calculated from the slopes and intercepts of the linear plot of ln ($q_e - q_t$) or (t/qt) against t respectively (Figures 17, and 18). It is seen that Azo Ligand adsorption is well described by the pseudo first order reaction kinetic. Moreover, the correlation coefficient (R^2) of first order reaction kinetic (0.8879) is higher than that of the second order reaction kinetic (0.5506) and greater value of rate constant for the adsorption data. (Table 8) shows the rate constants, q_e (experimental and calculated) and correlation coefficient (R^2) for pseudo first and second order reaction kinetic.

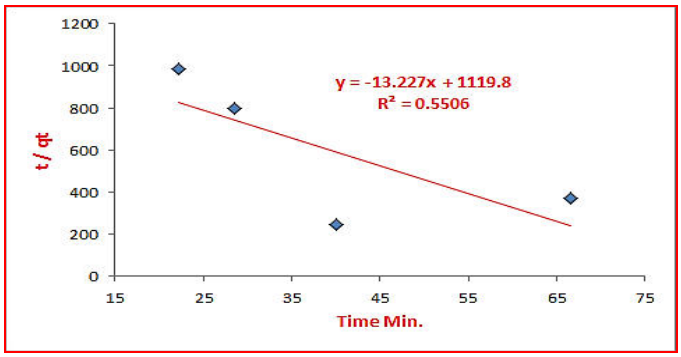

Figure 17.The pseudo-second-order kinetic models for the adsorption of 20 ppm. of Azo Ligand at (25±2) °C under optimum conditions.

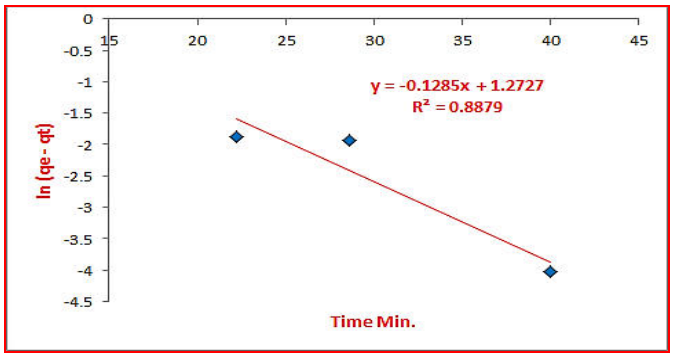

Figure 18, The pseudo-first-order kinetic models for the adsorption of 20 ppm. of Azo Ligand at (25±2) °C under optimum conditions.

Table 8.The pseudo - first and second- kinetic order parameters for the adsorption of 20 ppm. of Azo Ligand at (25±2) °C under optimum conditions.

qe Experimental (mg/g)	The pseudo-first-order kinetic models			The pseudo-second-order kinetic models		
0.1810	q_e calculated (mg/g)	K_1 (min^{-1})	R^2	q_e calculated (mg/g)	K_2 (g/mg/min)	R^2
	0.2800	0.1285	0.8879	0.0756	0.0051 x10^{-3}	0.5506

4. Conclusions

The present investigation shows that Iraqi initiated burned bentonite clay mineral (Montmorillonite) is an effective adsorbent for the removal of Azo Ligand from aqueous solutions (91.5 %). From the kinetic studies, it is observed that adsorption of Azo Ligand is very rapid in the initial stage and decreases while approaching equilibrium. The equilibrium time increases with initial Azo Ligand concentration. The percentage removal of Azo Ligand increases with the increase in adsorbent dosage and decreases with increase in initial Azo Ligand concentration. Experimental results are in good agreement with Langmuir, Freundlich and Temkin adsorption isotherm models, and have shown a good fitting to the experimental data. Adsorption of Azo Ligand obeys pseudo-first order equation with good correlation.

Acknowledgments
We would like to acknowledge Dean of the Faculty of Education Ibn al-Haitham, and the Chemistry department for their financial support.

References

[1]. Child R.G., Wilkinson R.G., Tomcu - Fucik A., (1977) Effect of substrate orientation of the adhesion of polymer joints. *Chem. Abstr*.; 87: p. 6031.
[2]. Garg H.G., Praksh C. (1972) Preparation of 4-arylazo-3, 5-disubstituted-(2H)-1, 2, 6-thiadiazine 1, 1-dioxides. *J. Med. Chem*.; 15(4) pp. 435-36.
[3]. Browing C.H., Cohen J.B., Ellingworth S., Gulbransen R., (1926). The antiseptic properties of the amino derivatives of styryl and anil quinoline. *Journal Storage*. 100: pp. 293-25. 1926.
[4]. Khalid A., Arshad M., Crowley D.E. (2008), Accelerated decolorization of structurally different azo dyes by newly isolated bacterial strains, *Appl. Microbiol. Biotech.* 78: pp 361-69.
[5]. Pagga U., Brown D. (1986). The degradation of dyestuffs in aerobic biodegradation tests. *Chemosphere*; 15: pp. 479-91.
[6]. Thoraya A., Farghaly, Abdallah ZA. (2008), Synthesis, azo-hydrazone tautomerism and antitumor screening of N-(3-ethoxycarbonyl-4, 5, 6, 7-tetrahydro-benzo[b]thien-2-yl)-2-arylhydrazono-3-oxobutanamide derivatives, *Arkivoc*.; 17: p. 295.
[7] Park Ch, Lim J, Lee Y, Lee B, Kim S, Lee J, Kim S.(2007). Optimization and morphology for decolorization of reactive black 5 by Funalia trogii. *Enzyme Microb. Tech*.; 40 :453; 1758-764.
[8]. Rajendra G.M., Madhu S.V., Naveen KS. (1998). Voltammetric investigations of the reduction of direct orange-31 a bisazo dye. *Croatica Chemica Acta*.; 71(3):pp.715-26.
[9]. Shridhari A.H., Keshavayya H., Hoskeri H.J., Ali RAS.(2011). Synthesis of some novel Bis 1,3,4-oxadiazole fused azo dye derivatives as potent antimicrobial agents. *Int. Res. J. Pure Appl. Chem.*; 1(3):pp. 119-29. 2011.
[10]. Chandravadivelu G., Senniappan P.(2011). In-vitro antimicrobial activity of novel derivative of azo dye from cyano ester. Int. *J. Res. Pharm. Chem*.; 1(4):pp. 1082-086.
[11]. Patel PS.(2012). Studies on synthesis and dyeing performance of disperse azo dyes based on Schiff base of ninhydrin and 3-amino phenol., *Arch. Appl. Sci. Res*.; 4(2):pp. 846- 51.
[12]. Chopde H.N., Meshram J.S., Pagadala R., Mungole A.J. (2010). Synthesis, characterization and antibacterial activity of some novel azo-azoimine dyes of 6-bromo-2-naphthol, *Int. J. Chem. Tech. Res.;* 2(3):pp. 1823-830.
[13]. Swati G., Romila K., Sharma I.K., Verma P.S. (2011). Synthesis, characterization and antimicrobial screening of some azo compounds, *Int. J. Appl. Biol. Pharm. Tech*.; 2(2):pp. 332-38.
[14]. Avci G.A., Ozkinali S., Ozluk A., Avci E., Kocaokutgen H.(2012). Antimicrobial activities, absorption characteristics and tautomeric structures of o,o'-hydroxyazo dyes containing an acryloyloxy group and their chromium complexes, *Hacettepe J. Biol. Chem.;*40 (2):pp. 119-26.
[15]. Gopalakrishnan S., Nevaditha N.T., Mythili C.V. (2011). Antibacterial activity of azo compounds synthesized from the natural renewable source, *Cardanol. J. Chem. Pharm. Res*.; 3(4):pp. 490-97.
[16] S.Y. Lee, S.J. Kim, S.Y. Chung and C.H. Jeong (2003) "Sorption of hydrophobic organic compounds onto organoclays", *Journal of Chemosphere (Oxford)*, 55, pp 781-785.
[17] Odom, I. E. (1984) "Smectite clay Minerals: Properties and Uses". *Philosophical Transactions of the Royal Society A: Mathematical, Physical and Engineering Sciences* 311 (1517): p. 391.
[18] Patterson, S.H and Murray, H.H. (1983). Clays. In: Lefond SI ed. Industrial minerals and rocks, 4th - Ed., *New York, American Institute of Mining, Metallurgical, and Petroleum Engineers*, pp. 519– 595.
[19] Bentonite, kaolin, and selected clay minerals. (*Environmental health criteria*; p 231), World Health Organization, Geneva, 2005.
[20] J. H. Potgieter (1991) Adsorption of Methylene Blue on activated carbon: an experiment illustrating both the Langmuir and Freundlich isotherms, *J. Chem.Educ.*68 (4) pp. 349- 350.
[21] Mohammed H. Abdul Latif, Ali Khalil Mahmood and Maha A. Al –Abayaji, (2012). Adsorption of thymol from aqueous solution using granulated surfactant modified Iraqi Na – 13montmorillonite clay, *Ibn Al-Haitham journal for pure and applied sciences*, vol. (25) no. 1; pp. 266 - 282.
[22] Amer J. Jarad, (2013). Synthesis and Characterization of 4-(4-Nitrobenzeneazo)- 3-Aminobenzoic acid complexes with Y (III) and La (III) ions, *Eur. Chem. Bull.*, 2(6), pp. .383 - 388.
[23] Nair, M.L.H., Sheela, A.(2008), Synthesis, Spectral, Thermal, and Electrochemical Studies of Oxomolybdenum (V), *Indian J. Chem*., 47A, pp.1787-1792.
[24] Robinson, R. A., and Stokes, R. H. (1968) "Electrolyte solutions", *2nd ed., rev. London, Butterworth's*.
[25] Zlem C .and Demet B. (2000). Adsorption of Some Textile Dyes by Hexadecyl trimethyl ammonium Bentonite, *J. of Turk Chem*., 25: pp. 193 - 200.
[26] Omer S. Alkhazrajy, Mohammed H. Abdul Latif and Maha A. Al-Abayaji, (2012), Adsorption of Metoclopromide Hydrochloride onto Burned initiated Iraqi bentonite, *Journal of Al- Nahrain University*, vol. 15(2); pp. .35 - 46.

[27] Agyei, N.M.; Strydom, C.A. and Potgieter, J.H., An investigation of phosphate ion adsorption from aqueous solution by fly ash and slag, Chem. and Concr. Res., 30 (5); pp. 823 - 826, 2000.
[28] Ho, Y.S. and McKay, G., Competitive sorption of copper and nickel ions from aqueous solution using peat., Adsorption-Journal of the International Adsorption Society, 5(4); pp. 409 - 417, 1999.
[29] Agyei, N.M.; Strydom, C.A. and Potgieter, J.H., An investigation of phosphate ion adsorption from aqueous solution by fly
[30] Baup , S.; Jaffre ,C.; Wolbert, D. and Laplanche, A., Adsorption of pesticides onto granulated activated carbon: determination of surface diffusivities using simple batch experiments., Adsorption; 6 (3); pp. 219 - 228, 2000.
[31] Wong, K.K.; Lee, C.K.; Low, K.S. and Haron, M. J., Removal of Cu and Pb by tartaric acid modified rice husk from aqueous solutions. Chemosphere, 50(1); pp. 23 - 28, 2003.